ACS APPLIED MATERIALS & INTERFACES

Letter

www.acsami.org

Visual Detection of DNA Mutation Using Multicolor Fluorescent Coding

Jinzhao Song, Qiong Yang,* Fengting Lv, Libing Liu, and Shu Wang*

Beijing National Laboratory for Molecular Science, Key Laboratory of Organic Solids, Institute of Chemistry, Chinese Academy of Sciences, Beijing, 100190, P. R. China

Supporting Information

ABSTRACT: A visual colorimetric method for detecting multiplex DNA mutations has been developed using multicolor fluorescent coding based on multistep FRET of cationic conjugated polymers. Expensive instruments and technical expertise are not required in this method. Also our visual system provides a quantitative detection by simply analyzing RGB values of images. Genomic DNAs extracted from 60 FFPE colon tissues can be sensitively determined by utilizing our visual assay with a high-throughput manner. Thus, it proves to be sensitive, reliable, cost-effective, simple, and high-throughput for mutation detection.

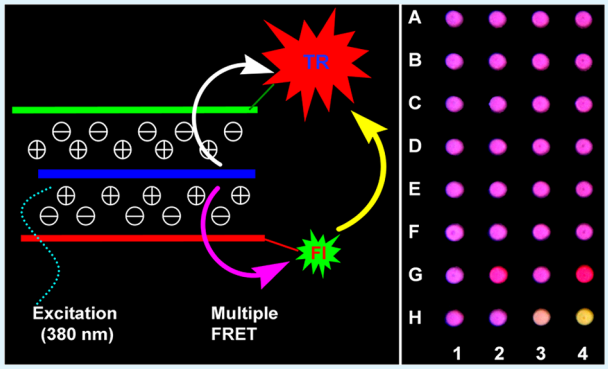

KEYWORDS: *conjugated polymers, FRET, DNA mutations, sensors, multicolor fluorescent coding*

1. INTRODUCTION

Detection of gene mutations (germline and somatic mutations) is clinically important for diagnostics, prognostics and disease assessment.[1] For this purpose, various methods have been reported, such as single strand conformation polymorphism analysis (SSCP),[2] high-resolution melting analysis (HRMA),[3] direct sequencing,[4] ARMS/Scorpion assay,[5] Taqman assay,[6] and SNaPshot assay.[7] However, these approaches require expensive instruments and technical expertise, which hinder their utility in poorly equipped rural areas. Compared with these methods, colorimetric detection of DNA mutation with visual readout mode exhibits significant advantages as it does not require expensive and complex analytical instruments to make it low cost, rapid to use and easy to operate. Commonly, colorimetric detection of DNA mutation is performed using DNA probe-modified or unmodified gold nanoparticles by target-induced aggregation.[8] However, these approaches cannot detect multiplex DNA mutations simultaneously in one tube, do not provide accurately quantitative analysis, and also have relatively lower detection sensitivity (picomolar). Thus, it is highly desirable to develop visual assay methods for simple, rapid, sensitive, and quantitative detection of DNA mutations.

Fluorescent technique is an extremely useful tool for improving detection sensitivity in comparison with colorimetric method. Also simultaneous detection of multiplex targets can be easily realized by multicolor probe coding.[9] In recent years, water-soluble cationic conjugated polymers (CCP) have attracted much attention in highly sensitive DNA detection.[10] They can amplify the fluorescence intensity of a tightly bound acceptor fluorophore by approximately 1 order of magnitude through an effective energy transfer pathway on excitation and only a trace amount of DNA is required (femtomolar). Particularly, the design of multistep fluorescence resonance energy transfer (FRET) between CCP and the different fluorescence dyes can realize multicolor tuning under single excitation wavelength.[11] Another important character of CCPs is that strong light emission from CCPs can be visualized with naked eyes under UV light irradiation, although it has not been adequately exploited for DNA detection.[12] This visual character exactly meets the requirement of point-of-care testing and molecular diagnostics in poorly equipped rural areas.[13] In this work, we developed a visual assay method for detecting multiplex DNA mutations using multicolor fluorescent coding based on multistep FRET of CCP. DNA mutations originated from practical clinical samples can be sensitively determined by utilizing our visual assay with a high-throughput manner.

2. RESULTS AND DISCUSSION

Cationic poly [(9,9-bis (6′-N, N,N- trimethylammonium)hexyl) fluorenylene phenylene] (CCP)[10e,f] and dNTPs respectively labeled with fluorescein and Tex Red (dUTP-Fl and dATP-TR) are used for multicolor fluorescent coding based on multistep FRET (see Scheme 1 for chemical structures) where CCP acts as the donor for fluorescein and Tex Red, fluorescein acts as the acceptor for CCP and the donor for Tex Red to satisfy the overlap integral requirement for FRET.[11] The PIK3CA gene

Received: May 11, 2012
Accepted: June 15, 2012
Published: June 15, 2012

Scheme 1. Schematic Representation of Visual Assay for Mutations in *PIK3CA* Gene and Chemical Structures of CCP, dUTP-Fl, and dATP-TR Used in the Assay. E545K is Located at Exon 9 and H1047R on Exon 20, and Blue Arrows show the Occurrence of Distance-Dependent Energy Transfer

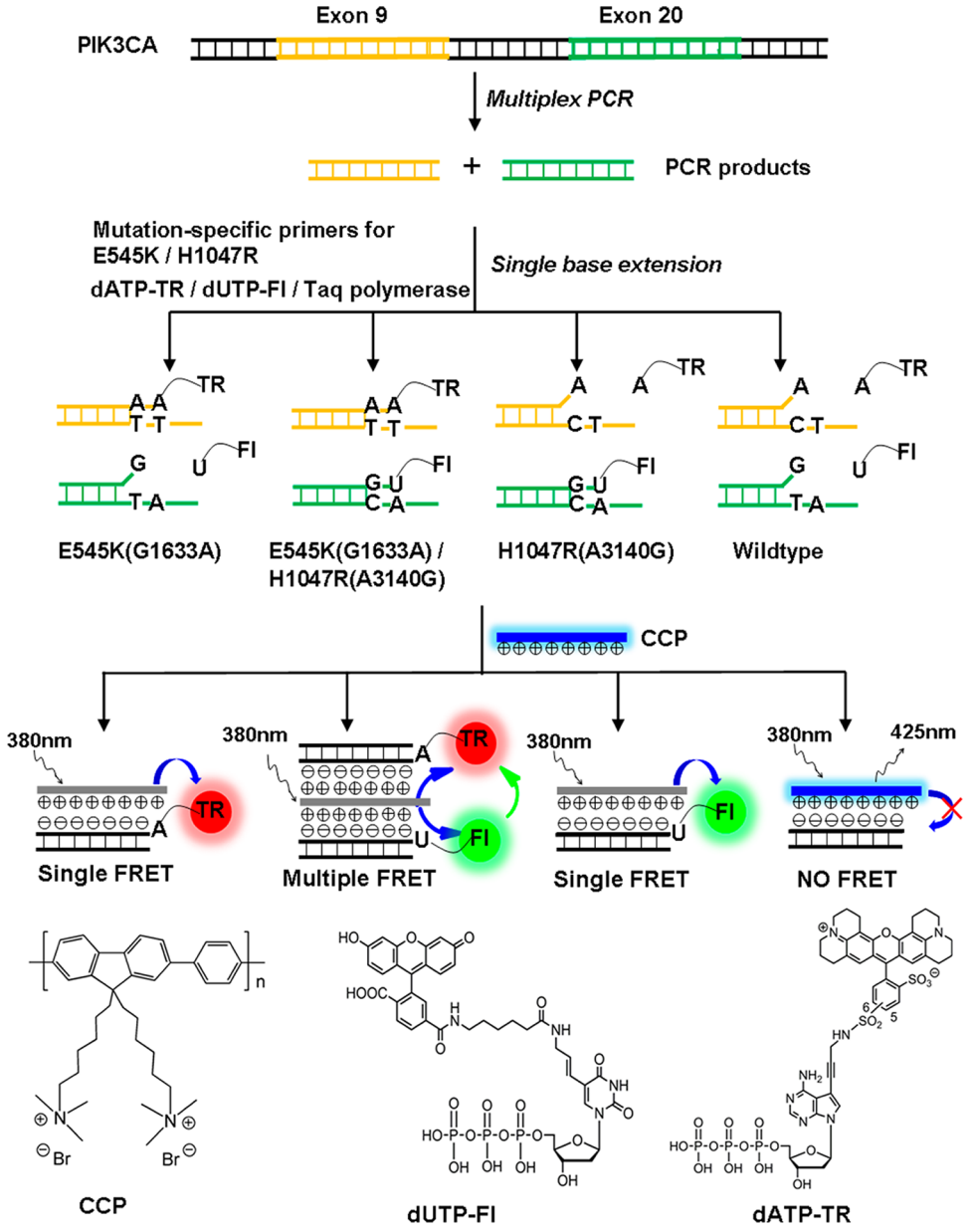

was chosen as detection target, which consists of four hotspot mutations: E542K (G1624A), E545K (G1633A) in exon 9 (helical domain), and H1047R (A3140G), H1047L (A3140T) in exon 20 (kinase domain). These mutations have been discovered in many different human cancers,[4b,14] thus, detection of PIK3CA mutations is of great significance not only for ongoing drug development but also for predicting response to cancer therapy.[15] The detection principle for the PIK3CA mutations is illustrated in Scheme 1. First, the multiplex PCR products were amplified from exons 9 and 20 of PIK3CA by two pairs of PCR primers (ex9-Fw/ex9-Rv, ex20-Fw/ex20-Rv), which contained four hotspot codon mutations (E545K, H1047R, E542K, H1047L). Second, two single-base extension (SBE) primers (E545K primer and H1047R primer) were used as probes to simultaneously detect two mutation sites in the amplified DNA fragments, E545K and H1047R, which are caused by a G→A base change at nucleotide position 1633 and a A→G base change at nucleotide position 3140, respectively. The 3′-terminal A base of E545K primer is complementary to the E545K mutation base but not to that of wildtype; meanwhile, the G base at the 3′-terminal of H1047R primer is complementary to the H1047R mutation base rather than the wildtype. The dATP-TR and dUTP-Fl and Taq polymerase are used for SBE reactions. In this detection system, there are four possible statuses: E545K, E545K/H1047R, H1047R, and wildtype. For E545K mutation, only dATP-TR is incorporated into the E545K primer, and upon addition of CCP, the strong electrostatic interactions between negatively charged DNA and cationic CCP bring them close to each other and efficient FRET from CCP to TR occurs upon exciting CCP with 380 nm. Similarly, for H1047R mutation, only dUTP-Fl can be incorporated into H1047R primer, leading to efficient

dx.doi.org/10.1021/am300830r | ACS Appl. Mater. Interfaces 2012, 4, 2885−2890

FRET from CCP to Fl. For the case of E545K/H1047R mutations, dATP-TR and dUTP-Fl are respectively incorporated into the E545K and H1047R primer, leading to multistep FRET (CCP→Fl, CCP→TR, and Fl→TR). For wildtype, the 3′-terminal bases of both E545K and H1047R primers are not complementary to the wildtype targets, and the base extension reactions cannot be performed. At this case, upon addition of CCP, weak electrostatic interactions between dATP-TR, dUTP-Fl and CCP can not keep them close enough, which results in inefficient FRET from CCP to TR or Fl. By triggering the emission color change of assay solution, it is possible to detect four possible statuses (three mutations and one wildtype) in one extension reaction. .

Figure 1a shows the emission spectra of extension products upon addition of CCP with the excitation wavelength of 380

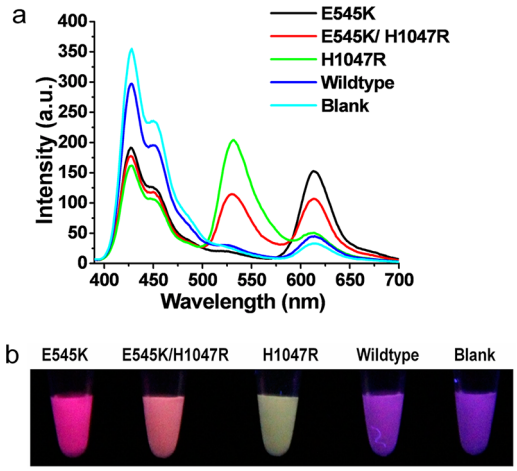

Figure 1. (a) Fluorescence spectra of E545K, E545K/H1047R, H1047R, and wildtype by mixing SBE products with CCP. SBE products were diluted by 100 times with HEPES buffer solution (25 mM, pH 8.0) before fluorescence measurement. [CCP] = 0.2 μM in RUs. The excitation wavelength is 380 nm. (b) The corresponding images of E545K, E545K/H1047R, H1047R, and wildtype when SBE products mixed with CCP (15 μM in RUs) in PCR tubes under 365 nm UV light irradiation. High-purity water was used as the blank.

nm, and Figure 1b shows the corresponding images of extension products mixed with CCP in PCR tubes under 365 nm UV light irradiation. High-purity water was used as blank. Two gDNA samples isolated from MCF-7 (E545K mutation), and T47D (H1047R mutation) breast cancer cell lines were serving as positive controls. For the blank, the emission maximum of CCP itself in HEPES buffer solution appeared at around 425 nm, and weak emission of TR at 613 nm was observed; therefore the solution exhibited bluish violet. For E545K mutation, efficient FRET from CCP to TR led to a significant quenching of CCP emission and an increase of TR emission, and the solution exhibited a pink color. For H1047R mutation, an evident emission of Fl was observed at 528 nm and the solution emitted a yellow-green color that composed of green emission of Fl and the bluish violet background. For both E545K and H1047R mutations, emissions of TR and Fl were observed and the solution displayed an orange-red color. In comparison to blank, a little higher TR and Fl fluorescence signals were demonstrated for wildtype sample due to a weak nonspecific extension reaction. However, these signals were much lower than that of specific extension reaction, and the solution exhibited a color similar to that of the blank. By directly observing the color of these solutions, we clearly distinguished three kinds of mutation status from the wildtype sample.

To assess the sensitivity and quantitative characteristic of our visual detection system, we mixed heterozygous mutant DNA from cell lines (MCF-7 or T47D) with wildtype DNA from non mutation cell line (293T) in various proportions. Photographs were taken by a digital camera and their quantitative data can be analyzed using red (R), green (G), and blue (B) values obtained from image-assay software (Adobe Photoshop). As demonstrated in Figure 2a,b, for E545K or H1047R mutation, as the proportion of mutant target in the test sample increases, R or G value of the images increases and B value decreases. Correspondingly, the emission intensity of TR or Fl increases and that of CCP decreases (see Figure S1a,b in the Supporting Information). For E545K/H1047R mutation, R and G values of the images increase and B value decreases when E545K/H1047R mutation proportion increases in the samples (Figure 2c), correspondingly, the emission intensity of TR and Fl increases and that of CCP decreases simultaneously (see Figure S1c in the Supporting Information). By observing color changes with naked eyes, 2% mutation level could be distinguished. Assay plots with various mutation proportions were drawn as functions of R/G/B ratios (R/B as x axis and G/B as y axis). As shown in Figure 2d, the R/B and G/B ratios increase with the increasing of E545K and H1047R mutation proportion in the tested samples, respectively. As expected, both R/B and G/B ratios increase when E545K/H1047R mutation proportion increases in the samples. As shown in the scatter diagram, we were able to detect E545K, E545K/H1047R and H1047R mutations by analyzing RGB value, even 2% mutation level could be distinguished from the total DNA. Correspondingly, assay plots with various mutation proportions as functions of FRET ratio ($I_{528\,nm}/I_{425\,nm}$ as y axis and $I_{613\,nm}/I_{425\,nm}$ as x axis) (Figure 2e) are consistent with those by analyzing RGB value. In addition, the relationships between different R/G/B ratios (such as R/B, G/B and (R+G)/B) and mutation proportions were investigated (see Figure S2 in the Supporting Information). The dynamic range of mutation proportion is from 2% to 100%, and all mutation proportions demonstrated reproducible results, which are identical to that of FRET ratios (see Figure S3 in the Supporting Information). By analyzing RGB values of the images, our FRET-based visual detection system can achieve excellent sensitivity and reproducibility as measuring the fluorescence spectra.

To investigate the application of our visual FRET-based assay on clinical samples, the genomic DNAs extracted from 60 FFPE colon tissues (30 adenocarcinomas and 30 adenomas samples) were assayed to determine the presence of four *PIK3CA* hotspot mutations. In these experiments, E545K and H1047R primers were grouped in one tube to detect E545K and H1047R mutation sites; E542K and H1047L primers were grouped in one tube to detect E542K and H1047L mutation sites. Cutoff values were established as the mean +3SD with R/B or G/B ratio values of negative control reactions and only samples with readout above these cutoff values were considered as positive signals. As presented in Figure 3a, four mutation samples were identified with naked eyes in 30 adenocarcinomas samples and the quantitative results obtained from the R/B and G/B scatter diagram were given in Figure 3b. The incidence of *PIK3CA* mutations in the samples was consistent with COSMIC database (catalogue of somatic mutations in cancer

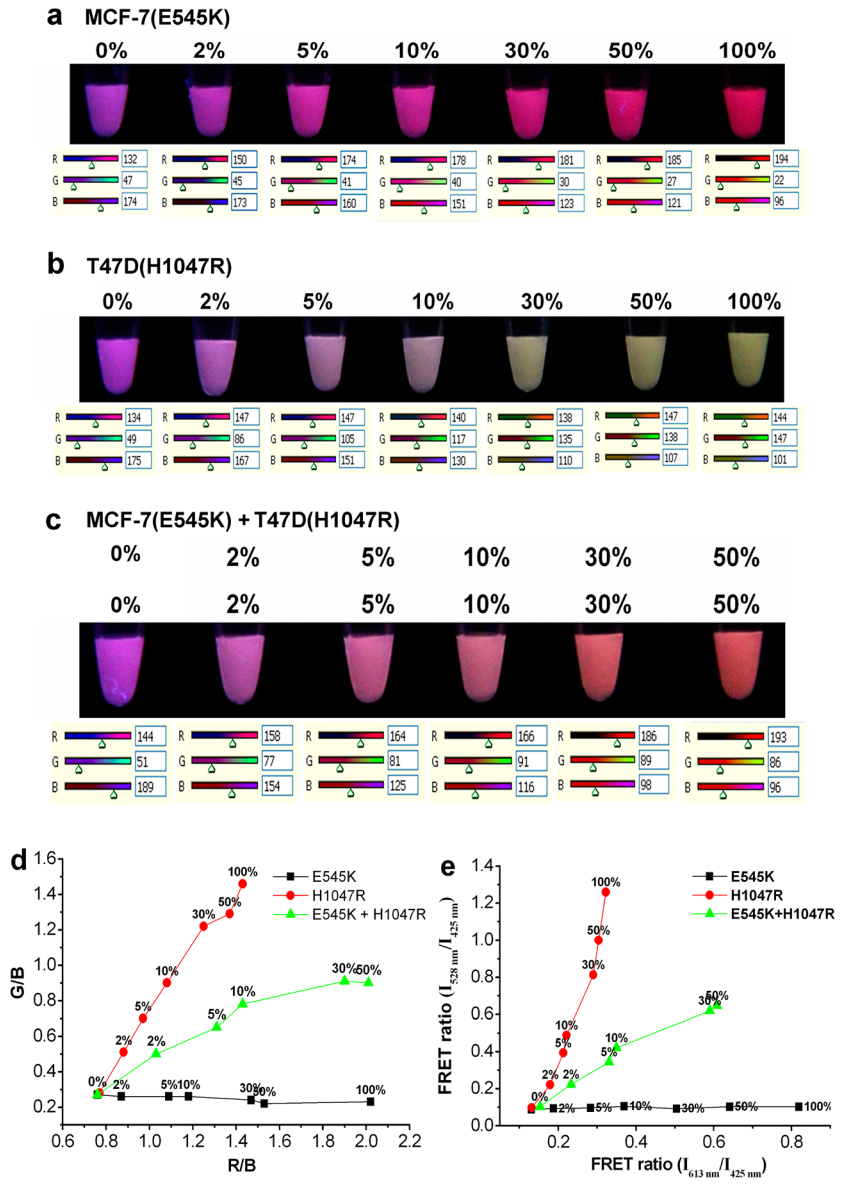

Figure 2. Visual detection of a series of extension products with various mutation proportions and the corresponding quantitative red (R), green (G), and blue (B) values obtained from image-assay software: (a) E545K, (b) H1047R, and (c) E545K/H1047R. Assay plots for E545K, E545K/H1047R, and H1047R with various mutation proportions as functions of (d) R/G/B ratios and (e) FRET ratios.

database). Of the colorectal samples positive for *PIK3CA* mutations, sample 15 (G2) was E545K, sample 24 (H3) was H1047R, and both sample 9 (B9) and sample 26 (A7) were E542K. To further verify our results, we measured fluorescence spectra and the FRET ratio scatter diagram was drawn (see Figure S4 in the Supporting Information). The fluorescence signals of mutation samples were significantly distinguished from that of wildtype samples, which was consistent with the results observed from visual experiments. This supports the tentative conclusion that visual FRET-based assay is a valid approach to efficiently detect DNA mutations in clinical samples. Furthermore, no mutations were detected in 30 adenomas samples either by observing the color changes or by measuring the fluorescence spectra (see Figure S5 in the Supporting Information).

DNA sequencing analysis, a gold standard for characterization of specific nucleotide alteration, was also performed to confirm the visual FRET-based results. As revealed in our sequencing results, sample 15, 24, and 26 were verified the presence of mutations. However, it is difficult to recognize mutation signals from the sequencing data of sample 9 (see Figure S6 in the Supporting Information). Board et al. reported that conventional sequencing was unable to detect the presence of E545K and H1047R mutations when their proportions were less than 30 and 50% of the total DNA, respectively.[5] Our experiments gave a quantitative result to estimate the percentage of tumor cells, and it was demonstrated that sample 15 and 26 consist of 30−50% mutations, sample 24 consists of 10−30% mutations, whereas sample 9 is composed of only about 5−10% mutations (Figure 2d). These results suggest that the visual FRET-based assay is more sensitive than DNA sequencing analysis and more *PIK3CA* mutations can be identified, and therefore the appearance of false-negative results can be efficiently avoided.

dx.doi.org/10.1021/am300830r | *ACS Appl. Mater. Interfaces* 2012, 4, 2885−2890

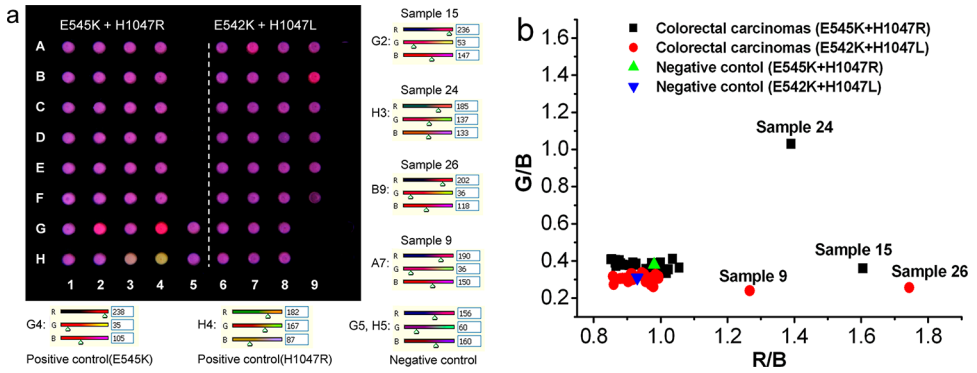

Figure 3. (a) Visual detection of 30 colon adenocarcinomas samples. On the left side of the white dotted line, E545K and H1047R primers were used to detect E545K and H1047R mutation sites. G4 and H4 are two positive controls (MCF-7 cell lines and T47D cell lines); G5 and H5 are two negative controls (293T cell lines). On the right side of the dotted line, E542K and H1047L primers were used to detect E542K and H1047L mutation sites. The 30 colon adenocarcinomas samples are identical to the left of dotted line. (b) Scatter diagram of mutation status from 30 colon adenocarcinomas samples, using R/B as *x* axis while G/B as *y* axis. The cutoff values of R/B and G/B ratios were 1.14 and 0.42 for the E545K and H1047R mutation, respectively, while 1.15 and 0.40 for E542K and H1047L mutation.

3. CONCLUSION

In summary, we developed a visual colorimetric method for detecting multiplex DNA mutations using multicolor fluorescent coding based on multistep FRET of cationic conjugated polymers. Compared to the visual methods reported previously, our assay system possesses several unique features. First, taking advantage of the amplification of fluorescence signals from CCP, high sensitivity was obtained and only a trace amount of DNA is required (femtomolar). As low as 2% mutant DNAs could be detected. Second, by triggering the emission color change of assay solution, it is possible to detect four possible statuses (three mutations and one wildtype) in one extension reaction, which streamlined workflow and reduced reaction time. Third, expensive instruments and technical expertise are not required in our method, some common equipment in biological laboratories and hospital pathologies, such as thermal cycler and UV viewing cabinet, are sufficient to accomplish the whole experiment procedure. Fourth, our system provides quantitative detection by analyzing RGB values of images with photoshop software. Finally, high-throughput analysis of genomic DNAs extracted from 60 FFPE colon tissues can be achieved by directly observing color changes of solutions in 96-well PCR plate under UV light irradiation. Our method proves to be sensitive, reliable, cost-effective, simple, and high-throughput for mutation detection. Therefore, it shows great potential application in clinical diagnosis, prognostics, disease prevention and risk assessment.

4. EXPERIMENTAL SECTION

FRET-Based Visual Detection and Fluorescence Measurement. Twenty-four microliters of CCP (15 μM) was added to the multiplex SBE products in PCR tubes or 96-well PCR plate followed by mixing thoroughly by pipetting, and then photographs were taken in a WD-9403F UV Viewing Cabinet under 365 nm UV light irradiation. In terms of the imaging of 96-well PCR plate, it is better to put the 96-well PCR plate upside down to make the UV light uniformly irradiate on the multiplex SBE products/CCP mixture. After taking the photographs, image-analysis software (Adobe Photoshop CS 8.0.1) was used to obtain the RGB values (R, G, and B are the red, green, and blue values, respectively). Six μL multiplex SBE products were diluted with 586 μL HEPES buffer (25 mM, pH 8.0) followed by adding 8 μL CCP (15 μM). The emission spectra were measured in a 3 mL quartz cuvette with an excitation wavelength of 380 nm.

■ ASSOCIATED CONTENT

Ⓢ Supporting Information

Experimental details and optical detection figures. This material is available free of charge via the Internet at http://pubs.acs.org/.

■ AUTHOR INFORMATION

Corresponding Author

*E-mail: wangshu@iccas.ac.cn (S.W.); yangqiong@iccas.ac.cn (Q.Y.).

Notes

The authors declare no competing financial interest.

■ ACKNOWLEDGMENTS

The authors are grateful to the National Natural Science Foundation of China (21033010, 21003140, 90913014, 21021091) and the Major Research Plan of China (2012CB932600, 2011CB935800).

■ REFERENCES

(1) Harris, T. J. R.; McCormick, F. *Nat. Rev. Clin. Oncol.* **2010**, *7*, 251.
(2) Inazuka, M.; Tahira, T.; Hayashi, K. *Genome Res.* **1996**, *6*, 551.
(3) Wittwer, C. T.; Reed, G. H.; Gundry, C. N.; Vandersteen, J. G.; Pryor, R. J. *Clin. Chem.* **2003**, *49*, 853.
(4) (a) Miyake, T.; Yoshino, K.; Enomoto, T.; Takata, T.; Ugaki, H.; Kim, A.; Fujiwara, K.; Miyatake, T.; Fujita, M.; Kimura, T. *Cancer Lett.* **2008**, *261*, 120. (b) Samuels, Y.; Wang, Z.; Bardelli, A.; Silliman, N.; Ptak, J.; Szabo, S.; Yan, H.; Gazdar, A.; Powell, S. M.; Riggins, G. J.; Willson, J. K. V.; Markowitz, S.; Kinzler, K. W.; Vogelstein, B.; Velculescu, V. E. *Science* **2004**, *304*, 554.
(5) Board, R. E.; Thelwell, N. J.; Ravetto, P. F.; Little, S.; Ranson, M.; Dive, C. L.; Hughes, A.; Whitcombe, D. *Clin. Chem.* **2008**, *54*, 757.
(6) Holland, P. M.; Abramson, R. D.; Watson, R.; Gelfand, D. H. *Proc. Natl. Acad. Sci. U.S.A.* **1991**, *88*, 7276.
(7) Hurst, C. D.; Zuiverloon, T. C. M.; Hafner, C.; Zwarthoff, E. C.; Knowles, M. A. *BMC Res. Notes* **2009**, *2*, 66.
(8) (a) Storhoff, J. J.; Elghanian, R.; Mucic, R. C.; Mirkin, C. A.; Letsinger, R. L. *J. Am. Chem. Soc.* **1998**, *120*, 1959. (b) Sato, K.; Hosokawa, K.; Maeda, M. *Nucleic Acids Res.* **2005**, *33*, e4. (c) Li, H. X.; Rothberg, L. J. *J. Am. Chem. Soc.* **2004**, *126*, 10958.

(9) (a) Medintz, I. L.; Uyeda, H. T.; Goldman, E. R.; Mattoussi, H. *Nat. Mater.* **2005**, *4*, 435. (b) Wang, L.; Tan, W. *Nano Lett.* **2006**, *6*, 84. (c) Yang, J.; Dave, S. R.; Gao, X. *J. Am. Chem. Soc.* **2008**, *130*, 5286.
(10) (a) Thomas, S. W.; Joly, G. D.; Swager, T. M. *Chem. Rev.* **2007**, *107*, 1339. (b) Ho, H. A.; Najari, A.; Leclerc, M. *Acc. Chem. Res.* **2008**, *41*, 168. (c) Duan, X.; Liu, L.; Feng, F.; Wang, S. *Acc. Chem. Res.* **2010**, *43*, 260. (d) Liu, B.; Bazan, G. C. *Chem. Mater.* **2004**, *16*, 4467.
(11) (a) Feng, X.; Duan, X.; Liu, L.; Feng, F.; Wang, S.; Li, Y.; Zhu, D. *Angew. Chem., Int. Ed.* **2009**, *48*, 5316. (b) Pu, K.-Y.; Zhan, R.; Liu, B. *Chem. Commun.* **2010**, *46*, 1470.
(12) (a) Xia, F.; Zuo, X.; Yang, R.; Xiao, Y.; Kang, D.; Vallée-Bélisle, A.; Gong, X.; Yuen, J. D.; Hsu, B. B. Y.; Heeger, A. J.; Plaxco, K. W. *Proc. Natl. Acid. Sci. USA* **2010**, *107*, 10837. (b) Duan, X.; Wang, S.; Li, Z. *Chem. Commun.* **2008**, *44*, 1302.
(13) Daar, S.; Thorsteinsdottir, H.; Martin, D. K.; Smith, A. C.; Nast, S.; Singer, P. A. *Nat. Genet.* **2002**, *32*, 229.
(14) Bader, G.; Kang, S.; Vogt, P. K. *Proc. Natl. Acad. Sci. U.S.A.* **2006**, *103*, 1475.
(15) Serra, V.; Markman, B.; Scaltriti, M.; Eichhorn, P. J. A.; Valero, V.; Guzman, M.; Botero, M. L.; Llonch, E.; Atzori, F.; Di Cosimo, S.; Maira, M.; Garcia-Echeverria, C.; Parra, J. L.; Arribas, J.; Baselga, J. *Cancer Res.* **2008**, *68*, 8022.